

XPS AND XANES STUDY OF LAYERED MINERAL VALLERIITE

Yu. L. Mikhlin¹, A. S. Romanchenko^{1*},
E. V. Tomashevich¹, M. N. Volochaev²,
and Yu. V. Laptev³

UDC 544.171.44:544.171.6

Mineral valleriite of the Talnakh deposit, which consists of alternating copper-iron sulfide layers and brucite-like layers of magnesium-aluminium hydroxide is studied for the first time by XPS at photon excitation energies ranging from 1.253 keV to 6 keV and CuL FeL, SL, AlL, MgK, and OK edge TEY XANES using synchrotron radiation. The comparison of the XPS and XANES spectra of valleriite and chalcopyrite, in particular, demonstrates that in the sulfide layers of valleriite, Cu⁺ and Fe³⁺ are in a tetrahedral coordination, however, a local positive charge on both cations is slightly lower than that in chalcopyrite, apparently, due to a structure disorder. The concentration of oxygen-bound iron decreases with an increase in the depth of the analyzed layer even after ion etching; probably, Fe does not enter into the brucite-like layer, but mainly forms its own surface structures.

DOI: 10.1134/S0022476617060105

Keywords: valleriite, high energy X-ray photoelectron spectroscopy, TEY XANES.

INTRODUCTION

Valleriite is sulfide-hydroxide mineral with a layered structure consisting of alternating nanosized brucite-like Mg and Al hydroxide and Cu–Fe–S sulfide layers [1–4] with a variable composition, which can be described by formula CuFeS₂·[1.31Mg(OH)₂·0.37Al(OH)₃]. However, the Cu and Fe ratio in the sulfide part and the Mg and Al ratio in the hydroxide part vary in a wide range, with iron substituting for magnesium and aluminum. Valleriite is relatively rare mineral, but its content in copper ores of the Norilsk group of copper-nickel deposits reaches 20% [1, 5, 6]. The flotation separation of these ores does not allow the recovery of more than 40–60% of copper and nickel into a sulfide concentrate, probably, due to intergrowth with serpentine and the specific surface properties of valleriite [5]. At present, not only the surface state but also the bulk structure of valleriite have been studied insufficiently. It is considered to be established that in the sulfide layers, copper (1+) and iron (3+) are in a tetrahedral coordination with sulfur anions as in chalcopyrite, however, they are randomly distributed over cation sites [2–4]. Based on the ⁵⁷Fe Mössbauer spectroscopy data, the authors of [7, 8] came to the conclusion that iron in the sulfide part is not only in the Fe³⁺ state, as in chalcopyrite, bornite Cu₅FeS₄, cubanite CuFe₂S₃ [9–16], but also in the 2+ oxidation state. In the brucite-like layers, iron is expected to be in the Fe²⁺ state in a tetrahedral

¹Institute of Chemistry and Chemical Technology, Siberian Branch, Russian Academy of Sciences, Krasnoyarsk, Russia; *romaas82@mail.ru. ²Kirensky Institute of Physics, Siberian Branch, Russian Academy of Sciences, Krasnoyarsk, Russia. ³Sobolev Institute of Geology and Mineralogy, Siberian Branch, Russian Academy of Sciences, Novosibirsk, Russia. Translated from *Zhurnal Strukturnoi Khimii*, Vol. 58, No. 6, pp. 1184–1190, July–August, 2017. Original article submitted November 23, 2016; revised January 30, 2017.

environment and Fe^{3+} in an octahedral environment of hydroxide ions [7, 8], however, it needs to be proved by other methods. The study of vallerite is complicated by difficulties in obtaining pure samples of natural minerals, which do not contain other phases (due to intimate intergrowth with serpentine, chalcopyrite, and other minerals) or synthetic compounds [2-4, 17]. The aim of the present work was to study natural Norilsk vallerite by X-ray photoelectron spectroscopy (XPS), including HAXPES, and XANES in soft energy ranges (up to 1400 eV). The CuL , FeL , SL XANES spectra of copper and iron sulfides were described in a series of works [9-14], but, as far as we know, XANES and HAXPES spectra of vallerite are absent in the literature. The simultaneous use of methods applying synchrotron radiation with different photon energies provided new information about the chemical state of elements and an insight into the surface state and bulk structure of vallerite.

EXPERIMENTAL

Natural vallerite from two different regions of the Talnakh deposit was used in the experiments; their spectra have no principal distinctions. The growth surface of the 2-3 mm sample was studied. The surface was wiped with a wet paper filter to remove fine particles or the mineral was ground in an agate mortar immediately before the transfer into the spectrometer chamber. Both types of the samples were fixed on a conducting double-sided adhesive carbon tape; the well reproducible spectra of minimally oxidized vallerites are described below. Polishing causes a substantial modification, including the oxidation of sulfide layers and surface contamination (by impurity serpentine, etc.); these spectra are not presented. The photoelectron spectra were recorded on a SPECS spectrometer with MgK_α radiation of the X-ray tube anode at a transmission energy of 20 eV for the survey spectra or 8 eV (narrow scans) of a PHOIBOS 150 MCD9 hemispherical energy analyzer. The HAXPES spectra were measured on a KMS-1 dipole channel (BESSY II, Helmholtz-Zentrum Berlin). Excitation radiation energies were varied from 2 keV to 6 keV using a double-crystal Si(111) monochromator [18]. The spectra were recorded using a Scienta R4000 energy analyzer optimized for high electron energies with a transmission energy of 200 eV for narrow scans, the electron emission angle of about 90°, and grazing incidence of the exciting beam. The binding energies were calibrated against the C1s line (285.0 eV); the spectra were fitted using the CasaXPS software package after the Shirley subtraction of a nonlinear background using the Gauss-Lorentz fitting of the peaks. The XANES spectra were obtained in the total electron yield (TEY) mode on the equipment of the Russian-German Laboratory at BESSY II; the details of the experiments are similar to those described in [15, 16].

RESULTS AND DISCUSSION

XPS. Table 1 lists the concentrations of main elements in the vallerite samples, which were determined by the X-ray microprobe analysis (EDS) on the surface using XPS with MgK_α radiation excitation (the carbon concentration caused mostly by hydrocarbon impurities of the surface was not taken into account). The surface is slightly enriched with magnesium, as for the rest, its composition is close to the bulk one. It is interesting that the calculations of the concentrations from the HAXPES data and taking into account the photoionization cross-section energy dependence, the energy analyzer transmission, and the escape depth [19, 20], did not allow us to get reasonable concentrations and the depth distribution of elements. We assume this to be due to a complicated morphology (mixing and mutual intergrowth of sulfide and hydroxide nanolayers, etc.) and a sophisticated mechanism of the photoelectron scattering [21].

TABLE 1. Concentrations of Elements in Vallerite, At%

Method	O	Al	Mg	S	Ca	Fe	Cu	Si	Ni
EDS	54.5	3.1	12.6	10.4	2.4	7.4	4.2	5.2	0.15
XPS	51	3	16	11	3.0	5.0	3.6	3.1	Traces

Fig. 1 shows the high resolution photoelectron spectra of copper and sulfur core lines in valleriite and, for comparison, in chalcopyrite, which were obtained under MgK_{α} excitation, i.e. more sensitive to the surface than HAXPES. The binding energy of the $Cu2p_{3/2}$ maximum is 932.6 eV, which is higher than that in chalcopyrite by 0.5-0.6 eV [15, 16, 19], however, the shake-up satellites are very weak in the range 944-948 eV (Fig. 1b), meaning that copper in valleriite has the 1+ oxidation state. The maximum of the $CuL_3M_{45}M_{45}$ Auger line is at the electron kinetic energy of 917.3 eV, whereas in chalcopyrite this energy is 918.0 eV. It is evidence of certain differences in the chemical state of copper in these minerals, although the modified Wagner parameter, which is equal to the sum of the $Cu2p_{3/2}$ binding energy and the kinetic energy of the Auger line, differs less. The spectra of copper are practically do not change with depth, excluding the broadening at a photon energy of 6 keV due to the deterioration of the monochromator resolution at high energies [19-21].

In the spectrum of sulfur of valleriite, the main component has a $S2p_{3/2}$ binding energy of 161.2 eV and corresponds to the monosulfide anion, and the intensity of the weak lines of di- and polysulfide forms at 162.6 eV and 163.2 eV is about 10% of total sulfur. In the spectrum of chalcopyrite, the contribution of high-energy lines is a bit higher. Di- and polysulfide anions are formed during oxidation of the surface of chalcopyrite and, probably, valleriite as a result of the formation of a metal-(predominantly iron-)deficit layer [15, 16, 19]. It can be mentioned that valleriite is more resistant to oxidation in the air than chalcopyrite, although it requires a more detailed study.

The spectra of iron (Fig. 2 shows the $Fe2p$ spectra measured at synchrotron radiation energies ranging from 2 keV to 6 keV) contain, at least, two components of the comparable intensity, which correspond to $Fe^{3+}-O$ (binding energies above 710 eV) and $Fe^{3+}-S$ with a binding energy of about 708 eV. The latter is in agreement with the predominance of Fe^{3+} in the sulfide layers as in chalcopyrite. The spectra have a complex multiplet structure, in particular, the $Fe(III)$ signal consists of four maxima and a satellite, in the case of several chemical forms of iron, their decomposition is ambiguous and is omitted here. It seems to be impossible to distinguish the forms of Fe^{2+} bonded to oxygen in the brucite-like layers and to sulfur in the sulfide part, on the contrary to that supposed in [7, 8]. When the analysis depth increases, the $Fe^{3+}-S$ fraction increases steadily, thus demonstrating that oxidized iron is located in the near-surface layers.

The $O1s$ spectrum has a line with a binding energy (BE) of 529.9 eV, which slowly decreases with increasing excitation energy. This line is typical of O^{2-} in iron oxides, although this form of oxygen must be absent in the brucite-like layer; hydroxide groups produce a line with BE of 531.5 eV. Probably, at least a part of oxidized iron forms its own oxide (oxyhydroxide) phase rather than enters into the hydroxide layers. In principle, the impurity of oxides, e.g., magnetite, can be initially present in the sample, but not in such a high concentration. Therefore it seems very likely that iron oxide is formed on the surface as a result of the oxidation of the sulfide layers of the mineral.

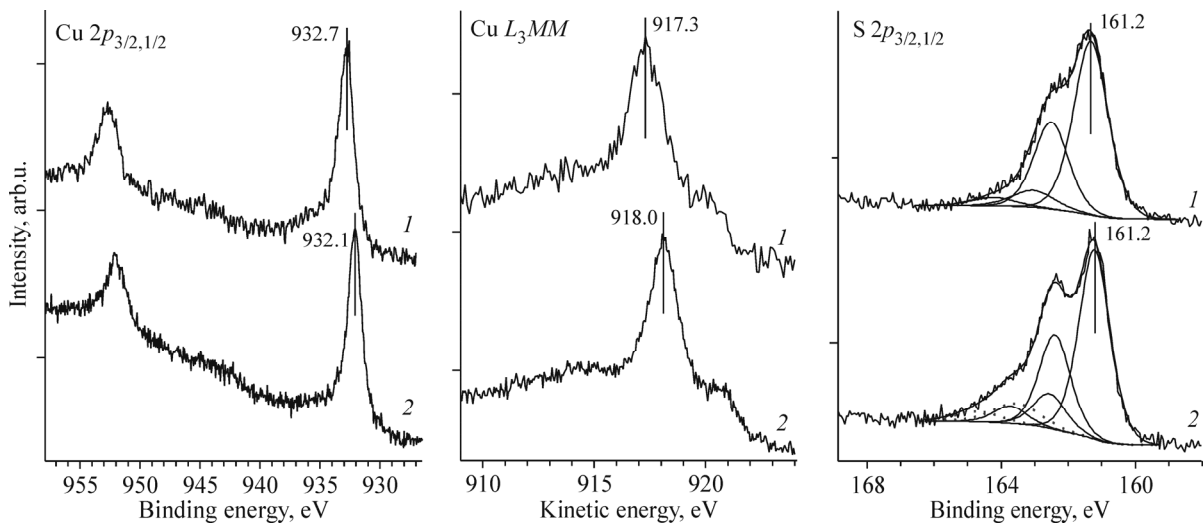


Fig. 1. XPS spectra of valleriite (1) and chalcopyrite (2) obtained with MgK_{α} radiation excitation (1253.6 eV).

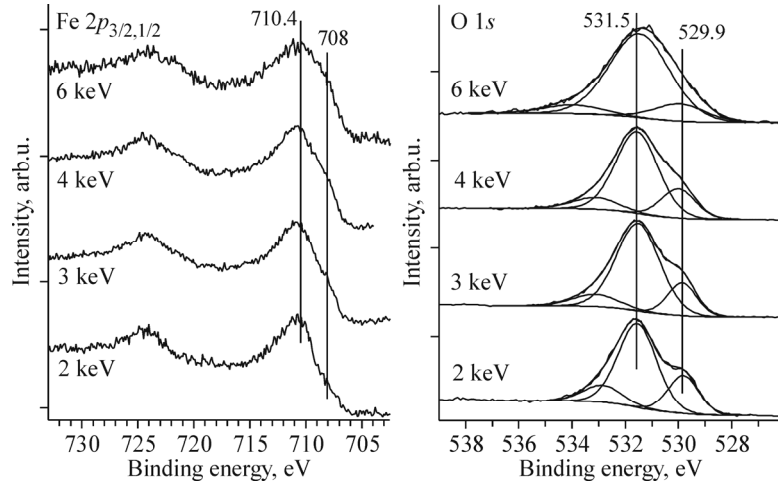


Fig. 2. XPS spectra of iron and oxygen in valleriite, obtained with synchrotron radiation excitation at photon energies of 2 keV, 3 keV, 4 keV, and 6 keV.

X-ray absorption spectroscopy. Fig. 3 shows the L edge TEY XANES spectra of copper, iron and sulfur of valleriite and, for comparison, chalcopyrite, as well as Mg L and OK edge TEY XANES spectra of valleriite. The Cu L edge spectrum of valleriite, as well as that of chalcopyrite, has a prepeak with an energy of 932.6 eV, which is responsible for the transitions of Cu $2p$ electrons to the unoccupied 3d orbitals. Although formally copper has a Cu d^{10} configuration, the prepeak height is higher than the maximum of the absorption jump (936 eV), because the probability of the electron transition to 3d is much higher than that to the s states. The prepeak of valleriite is slightly lower than that of chalcopyrite, which indicates a larger number of electrons located on the Cu3d orbitals, however, it is higher than that in bornite [9, 16]. The shape of the

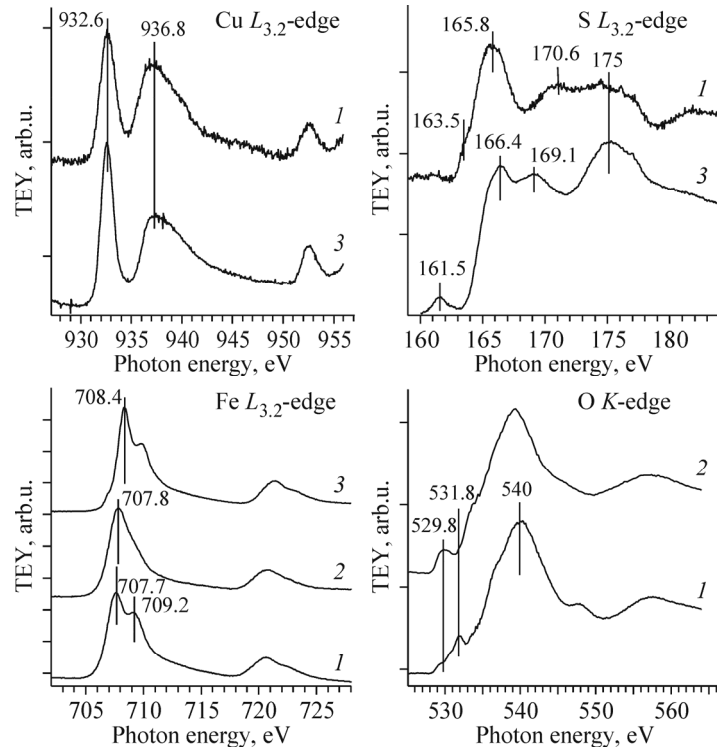


Fig. 3. Cu $L_{2,3}$, SL $_{2,3}$, Fe $L_{2,3}$ and OK edge TEY XANES spectra of valleriite (1, 2) and chalcopyrite (3); after 10 min Ar $^+$ (2) ion etching.

spectrum in the post-edge region slightly differs from that of chalcopyrite, i.e. the chemical state of copper in these minerals is nearly the same.

The spectra of sulfur have pronounced distinctions from the SL edge spectra of chalcopyrite. A small prepeak at 163.5 eV, forbidden by the selection dipole rules, is in accordance with the $S2p \rightarrow Fe^{3+}3d + S3s/3p$ transitions [12], and is close in energy to the similar maximum in bornite (about 163 eV [16]), meanwhile in the spectrum of $CuFeS_2$, it has an energy of 161.5 eV [24, 25]. The most pronounced absorption peak corresponding to the $S2p \rightarrow S3s/3p$ transitions, is located at an energy of about 166 eV, as in chalcopyrite. The resonances at 170.6 eV (at 169.1 eV in chalcopyrite) and ~175 eV are attributed to transitions to the $S3d (e)$ and $S3d (t_2)$ states respectively [15, 16]. Thus, the differences in the spectra can be explained by a smaller splitting of unoccupied $S3d$ orbitals in valleriite (about 4.4 eV), than that in chalcopyrite (5.5 eV), bornite Cu_5FeS_4 (6.5 eV), or cubanite $CuFe_2S_3$ (5.6 eV) [9, 12, 16].

The shape of the $FeL_{2,3}$ edge spectrum is typical of Fe^{3+} in a tetrahedral environment, but the main peak is shifted to lower energies as compared to that in chalcopyrite, which supposes a higher electron density (a less positive charge) on the Fe atoms. The distinctions in the $FeL_{2,3}$ edge spectra are partially explained by a higher content of $Fe^{3+}-O$ bonds that contribute to the second maximum with an energy of 709.2 eV. After Ar^+ ion etching (accelerating voltage of 2.9 kV), which removes about 3-5 nm of the surface layer, the peak intensity drops. Thus, it can be concluded that, in accordance with the HAXPES data, $Fe(III)$ oxyhydroxides are located predominantly on the surface and do not enter into the brucite part of the composite. In the NiL_3 edge spectrum (it is omitted in Fig. 4), the main absorption peak has an energy of ~852.5 eV, which shows that in the sulfide layers nickel is in the 2+ oxidation state [22]. The impurity manganese is bonded mostly to oxygen.

In the OK edge spectra, the main features with the energies of 540 eV, 548 eV, and 558 eV are typical of brucite [23], and the prepeaks with the energies of about 530 eV and 532 eV seem to be attributed to iron oxyhydroxides [24]. They are removed by ion etching, and the peak at 531.8 eV nearly disappears, whereas the prepeak at 529.8 eV remains and even slightly increases. The latter, as described in [25], is explained by radiation damages (ion bombardment) of the lattice of oxides and hydroxide, in this case, magnesium hydroxide (the brucite layer).

The MgK and AlL edge spectra of valleriite, which were not earlier published, were also measured. The shape of the spectrum of magnesium (the low-level signal/noise ratio is explained by a low monochromator transmission at these energies) is very close to that of brucite $Mg(OH)_2$ [24]. In the $AlL_{2,3}$ edge XANES spectra, the A peak has an energy of 77.5 eV, which is characteristic of silicate glasses, and the position of the B peak (79.8 eV) is more typical of aluminum with coordination number 4 [26]; some fine details of the spectrum are due to the $Al2p$ spin-orbit splitting (about 0.4 eV). However, the conclusions about the aluminum state in the brucite-like layers of valleriite are insufficiently proved by these spectra because the sample under study contains serpentine and other aluminosilicate impurities.

Thus, the comparison of the XPS and TEY XANES spectra of valleriite demonstrates that in the sulfide layers copper and iron are in the formal oxidation state of 1+ and 3+ respectively, but the local positive charges on both cations are slightly smaller than those in chalcopyrite, which is likely to be due to the less ordered structure. Oxygen-bound iron, as a rule, does not enter into the brucite-like layer phase but forms its own surface structure, probably, as a result of sulfide

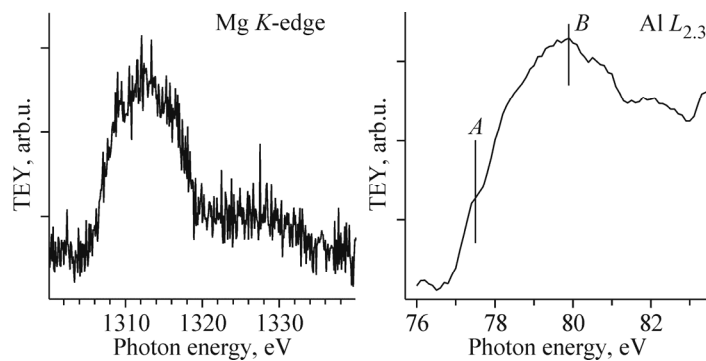


Fig. 4. MgK and $AlL_{2,3}$ edge TEY XANES spectra of valleriite.

oxidation. Nevertheless, the sulfide component exhibits comparable or even greater oxidation stability in comparison with that in chalcopyrite.

CONCLUSIONS

The XPS methods with photon excitation ranging from 1.253 keV to 6 keV and X-ray absorption spectroscopy in the soft energy region were used to study a natural nanocomposite – valleriite, consisting of alternating copper-iron sulfide layers and brucite-like layers of magnesium-aluminum hydroxide. The sample contained serpentine and aluminosilicate impurities, which complicated the study of the hydroxide component of the mineral. The comparison of the X-ray microprobe analysis and XPS data has demonstrated a minor enrichment of the surface layers with magnesium. The depth distribution of the elements has not been determined by HAXPES, probably, because of the complicated nanosized morphology of the material. The combined analysis of the XPS and XANES spectra of valleriite is consistent with that in the sulfide layers copper and iron are in the tetrahedral coordination and have formal oxidation states 1+ and 3+ respectively. The local positive charges on both cations are slightly smaller than those in chalcopyrite, which seems to be due to the structure disorder. The oxygen-bound iron(3+) does not enter into the brucite-like layer phase, but mostly forms its own surface structures.

The work was supported by the Russian Science Foundation (grant No. 14-17-00280) and the bilateral program “Russian-German Laboratory at BESSY-II”.

The authors express their gratitude to the Helmholtz Zentrum Berlin for time provision at the RGLab and HIKE stations and to the personnel of the Stations for their assistance in the running of the experiments.

REFERENCES

1. A. D. Genkin, V. V. Distler, and G. D. Gladyshev, *Metallogeny of the Taimyr-Norilsk Region*, Nauka, Moscow (1981).
2. H. T. Evans and R. Allman, *Zeitschrift fur Kristallogr.*, **127**, 73-93 (1968).
3. A. E. Hughes, G. A. Kakos, T. W. Turney, and T. B. Williams, *J. Solid State Chem.*, **104**, Iss. 2, 422-436 (1993).
4. R. Li and L. Cui, *Int. J. Miner. Process.*, **41**, 271-283 (1994).
5. D. C. Harris, L. J. Cabry, and J. M. Stewart, *Am. Miner.*, **55**, 2110-2114 (1970).
6. D. A. Dodin, *Nickel-Sulfide Ores of the Norilsk Deposits* [in Russian], Nauka, Saint-Petersburg (2002).
7. N. I. Chistyakova, T. V. Gubaidulina, and V. S. Rusakov, *Czech. J. Phys.*, **56**, 123-131 (2006).
8. T. V. Gubaidulina, N. I. Chistyakova, and V. S. Rusakov, *Bull. Russ. A. Sci.: Physics.*, **71**, No. 9, 1269-1272 (2007).
9. S. W. Goh, A. N. Buckley, W. M. Skinner, and L. J. Fan, *Phys. Chem. Miner.*, **37**, 389-405 (2010).
10. O. Sipr, P. Machek, and A. Simunek, *Phys. Rev. B*, **69**, Iss. 15, 155115 (2004).
11. J. Petiau, Ph. Sainctavit, and G. Calas, *Mater. Sci. Eng. B*, **1**, 237-249 (1988).
12. D. Li, G. M. Bancroft, M. Kasrai, M. E. Fleet, X. H. Feng, B. X. Yang, and K. H. Tan, *Phys. Chem. Miner.*, **21**, 317-324 (1994).
13. Ph. Sainctavit, J. Petiau, A. M. Flank, J. Ringeissen, and S. Lewonczuk, *Phys. B*, **158**, 623/624 (1989).
14. E. V. Korotaev, M. M. Syrovashin, N. N. Peregudova, V. V. Kanazhevskii, L. N. Mazalov, and V. V. Sokolov, *J. Struct. Chem.*, **56**, No. 3, 596-600 (2015).
15. Y. L. Mikhlin, Y. V. Tomashevich, I. P. Asanov, A. V. Okotrub, V. A. Varnek, and D. V. Vyalikh, *Appl. Surf. Sci.*, **225**, 395-409 (2004).
16. Y. Mikhlin, Y. Tomashevich, V. Tauson, D. Vyalikh, S. Molodtsov, and R. Szargan, *J. Electron Spectrosc. Relat. Phenom.*, **142**, 85-90 (2005).
17. Yu. V. Laptev, V. S. Shevchenko, and F. Kh. Urakaev, *Hydrometallurgy*, **98**, 201-205 (2009).
18. Yu. Mikhlin, Ye. Tomashevich, S. Vorobyev, S. Saikova, A. Romanchenko, and R. Félix, *Appl. Surf. Sci.*, **387**, 796-804 (2016).

19. Y. Mikhlin, V. Nasluzov, A. Romanchenko, Y. Tomashevich, A. Shor, and R. Félix, *Phys. Chem. Chem. Phys.*, **19**, 2749-2759 (2017).
20. S. Tanuma, H. Yoshikawa, H. Shinotsuka, and R. Ueda, *J. Electron Spectrosc. Relat. Phenom. B*, **190**, 127-136 (2013).
21. M. Gorgoi, S. Svensson, F. Schäfers, and G. M. Öhrwall, *Nucl. Instrum. Methods A.*, **601**, 48-53 (2009).
22. J. F. W. Mosselmans, R. A. D. Pattrick, G. van der Laan, J. M. Charnock, D. J. Vaughan, C. M. B. Henderson, and C. D. Garner, *Phys. Chem. Miner.*, **22**, 311-317 (1995).
23. P. A. van Aken, Z. Y. Wu, F. Langenhorst, and F. Seifert, *Phys. Rev. B*, **60**, 3815-3820 (1999).
24. P. A. van Aken, B. Liebscher, and V. J. Styrsa, *Phys. Chem. Miner.*, **25**, 494-498 (1998).
25. L. J. Garvie, *Am. Miner.*, **95**, 92-97 (2010).
26. C. Weigel, G. Calas, L. Cormier, L. Galoisy, and G. S. Henderson, *J. Phys.: Condens. Matter.*, **20**, No. 13, 135219 (2008).